ORIGINAL PAPER

From rocks to ore

B. Lehmann · A. Dietrich · A. Wallianos

Abstract Metal enrichment to ore grade is the ultimate outgrowth of large-scale and long-term fractionation processes of the thermally driven and unique water-cooled geological evolution of the Earth. Silicic magmatism along convergent margins is the most important lithospheric fractionation process for the formation of the continental crust and porphyry/intrusion-related ore deposits. Reconnaissance microanalysis of melt inclusions from Central Andean porphyry systems refines a metallogenic model for copper–gold and tin porphyry mineralization. Magmatic mixing and early exsolution of a fluid phase are important ingredients for porphyry Cu–Au systems in association with silicic rocks of moderate levels of fractionation (such as diorites and monzonites), whereas extended magmatic fractionation with late-stage fluid evolution characterize lithophile-element-enriched tin porphyry systems.

Key words Metallogeny · Ore deposits · Porphyry systems · Central Andes · Melt inclusions

General background: Global fractionation trends and major geochemical reservoirs

The chemical dynamics of the Earth is controlled by a few fundamental petrological processes which are behind the formation of a number of global chemical reservoirs with specific element-distribution patterns. These reservoirs provide the chemical and physical background for magmatic, hydrothermal and sedimentary redistribution processes. The ultimate outcome of these fractionation processes at very advanced stages is local metal enrichment to ore grade as a complementary feature of large-scale metal depletion in individual geochemical reservoirs (Brimhall 1987). Extreme reaction progress of petrological processes characterizes ore deposits as the end members of the general rock spectrum. An understanding of these fractionation processes allows a sound target definition in mineral exploration.

Figure 1 summarizes the geochemical history of the Earth and shows the behaviour of numerous elements. It is generally believed that Type-1 carbonaceous chondrites (CI) closely approximate the condensable fraction of primordial solar system material because the element pattern of the photosphere of the sun and of CI chondrites is very similar (Anders and Grevesse 1989). The accretion of the Earth appears to have taken place heterogeneously from several chemically different components (Palme and O'Neill 1996). Accretion was accompanied by the release of kinetic and gravitational energy with large-scale melting and evaporation. Refractory-volatile fractionation led to enrichment of refractory components in the Earth and other planets of the inner part of the solar system (Taylor 1992). Volatile components became concentrated in the outer solar system. Core segregation happened within the first 100 Ma of Earth's history leading to preferential partitioning of siderophile elements into the core (Allègre et al. 1995). This metal–silicate fractionation resulted in dramatic depletion of the platinum-group elements and gold in the silicate portion of the Earth (McDonough and Sun 1995). Archean crust formation and intracrustal differentiation, both by crystal–liquid fractionation, led to the present-day geochemical pattern of the continental crust with enrichment of incompatible components in the upper crust. The mass ratio of mantle/crust of

B. Lehmann (✉) · A. Dietrich
Institut für Mineralogie und Mineralische Rohstoffe,
Technische Universität Clausthal, Adolph-Roemer-Strasse 2A,
D-38678 Clausthal-Zellerfeld, Germany
e-mail: lehmann@min.tu-clausthal.de
Tel.: +49-5323-722776
Fax: +49-5323-722511

A. Wallianos
Max-Planck-Institut für Kernphysik, Saupfercheckweg 1,
D-69029 Heidelberg, Germany

Fig. 1 Fractionation pattern of some elements during the Earth's history. Data mostly from GERM (1998), and Morgan and Anders (1980). Adapted from Lehmann (1994). End of primitive Earth stage is defined by Xe closure age of 4.45 ± 0.02 Ga (Zhang 1998)
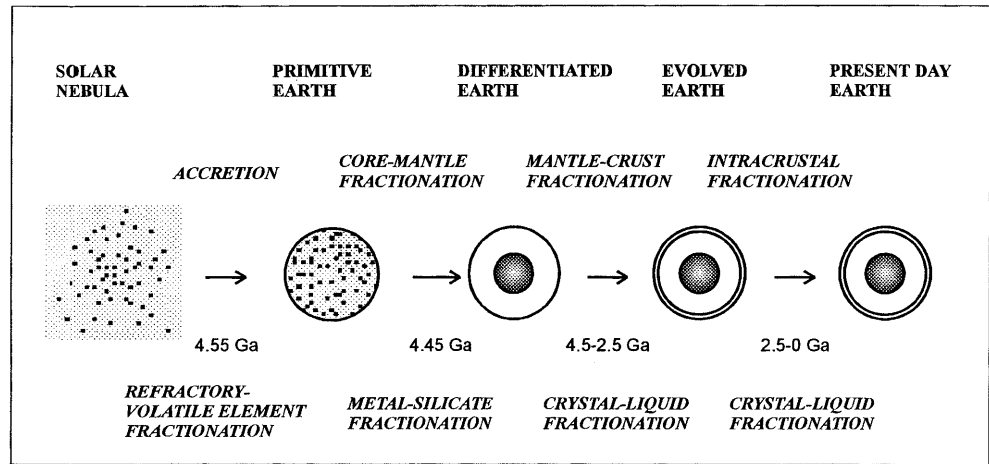
24 Cr	2660 ppm	4120 ppm	2625 ppm	120 ppm	215 ppm	35 ppm
29 Cu	126 ppm	31 ppm	30 ppm	26 ppm	26 ppm	25 ppm
42 Mo	0.928 ppm	2.35 ppm	0.05 ppm	0.65 ppm	0.45 ppm	1.5 ppm
50 Sn	1.72 ppm	0.39 ppm	0.13 ppm	1.5 ppm	1.1 ppm	2.5 ppm
73 Ta	0.014 ppm	0.023 ppm	0.037 ppm	0.7 ppm	0.6 ppm	0.96 ppm
74 W	0.093 ppm	0.18 ppm	0.029 ppm	0.69 ppm	0.5 ppm	2.0 ppm
78 Pt	0.99 ppm	1.67 ppm	0.007 ppm	0.0018 ppm	0.0019 ppm	0.0015 ppm
79 Au	0.140 ppm	0.26 ppm	0.001 ppm	0.003 ppm	0.0014 ppm	0.0018 ppm
82 Pb	2.5 ppm	0.115 ppm	0.15 ppm	12.5 ppm	4.3 ppm	20 ppm
92 U	0.008 ppm	0.014 ppm	0.02 ppm	1.4 ppm	0.28 ppm	2.8 ppm
Rb/Sr	0.295	0.032	0.028	0.17	0.03	0.32

approximately 170 limits the enrichment factor of near-perfectly incompatible components such as rubidium, lead, tantalum or uranium in the continental crust (Fig. 2).

Most elements are incompatible with respect to the major mantle minerals, and become enriched in the crust. Only a few elements are enriched in the mantle, such as Mg, Cr, Ni, Te and the platinum-group elements (Fig. 2). These elements form ore deposits in mantle environments or in direct relationship to mantle processes.

Continental crust is a specific feature of the Earth. The formation of continents requires the production of vast amounts of felsic igneous rocks. Subduction of an even vaster amount of hydrated oceanic crust over an extended period of geological time provides an effective mechanism (Cox and Hart 1986). This is probably possible only where a large percentage of the surface area of a planet is covered by liquid water, i.e. oceans (Campbell and Taylor 1983). The Earth is the only known planet with present-day P–T conditions allowing liquid water on its surface (Fig. 3).
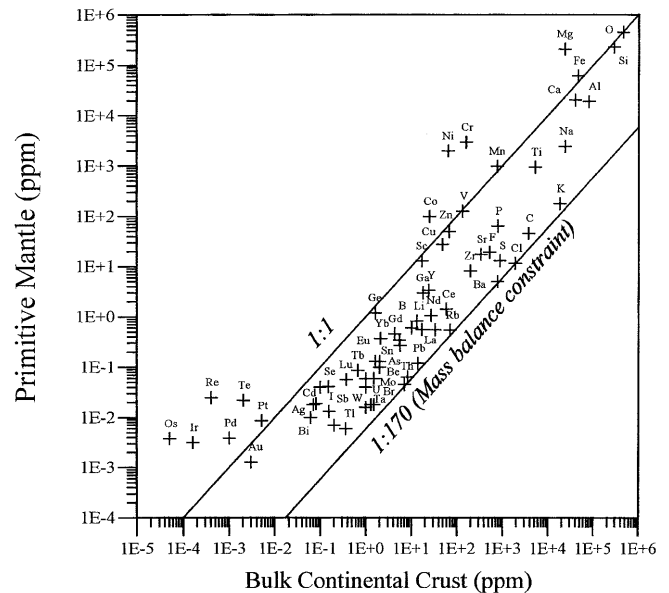

Fig. 2 Bulk continental crust vs primitive mantle. The mantle/crust mass ratio defines the upper limit of incompatible element enrichment of approximately 170 in continental crust. Data from Taylor and McLennan (1985) and Wedepohl (1995)

Hot and cold water: metal redistribution

The most efficient metal transport in ore formation is by aqueous fluids (ocean and meteoric water to hydro-carbo-thermal systems). Minerals dissolve in aqueous fluids through the formation of aqueous species in the form of simple ions or, much more importantly, complexes (Helgeson 1964). Most mineral components have prograde solubilities, and magmatic-hydrothermal systems require orders of magnitude less fluid flow compared with low-temperature deep-sea circula-
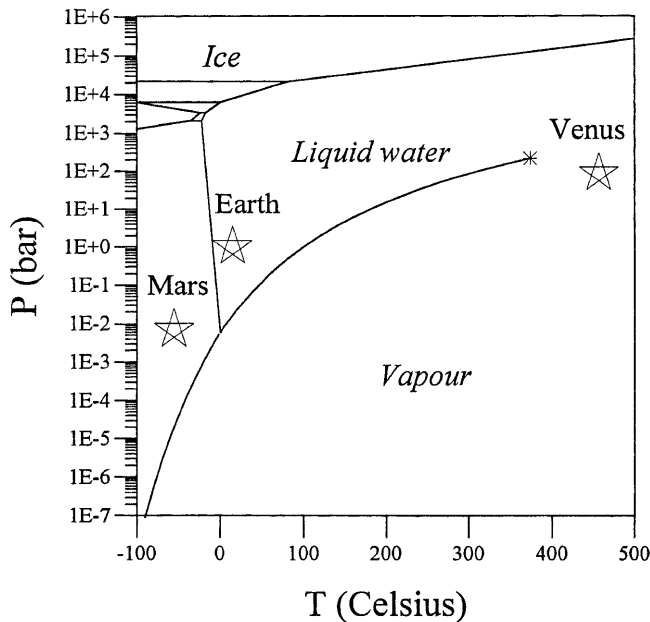
Fig. 3 Pressure–temperature phase diagram for water and average surface P–T conditions of terrestrial planets. Present-day P–T conditions allow liquid water only on the Earth's surface

tion for the same amount of metal throughput (Fig. 4). The main fluid reservoir are the oceans which are recycled through the continental crust via atmospheric and subduction processes. Fluid flow in the lithosphere is controlled by thermal gradients and permeability. Maximum fluid flow needs high heat flow and
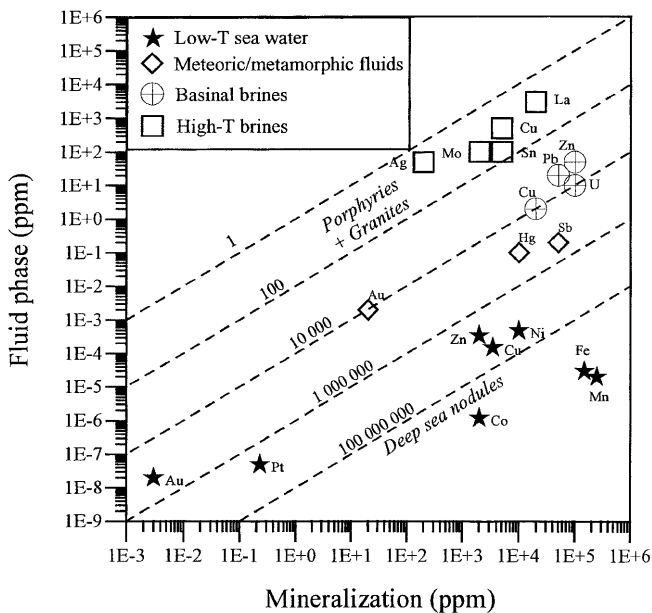

Fig. 4 Metal content in selected fluid phases vs ore grade. Seawater data from Nozaki (1997). Other data from a variety of sources. Lanthanum (La) refers to hydro-carbo-thermal systems related to carbonatites (Bühn and Rankin 1999)

extensional tectonic activity. Such conditions characterize convergent and divergent plate boundaries (magmatic arcs with intrusion-related ore deposits; Sillitoe 1997), as well as intracontinental shear zones (orogenic lode-gold deposits; Groves 1993) and rift zones (U–Au–Cu deposits, kimberlites and carbonatites; Mitchell and Garson 1981).

The metal transport capability of the fluid phase and its flow rate define the scale of ore-forming systems. Simple "back-of-the-envelope" calculations show that ore deposits must have several-orders-of-magnitude larger fluid systems associated. An indication of the fluid volume responsible for the formation of hydrothermal ore deposits can be derived from the quantity of hydrothermal quartz precipitated because the logarithm of quartz solubility is linearly dependent on $1/T$ (temperature), but below the critical point nearly independent of ionic strength, pH and pressure (Holland 1967). According to this estimate, the amount of hydrothermal quartz in mesothermal/epithermal systems requires on the order of 1000 times more fluid.

Large-scale metal depletion is difficult to detect and little documented. This must be due to the relatively low efficiency of bulk metal leaching which often results in deficiency patterns not easy to distinguish from the general log-normal distribution pattern of trace elements.

An example for relatively efficient metal leaching in apical portions of a tin granite system is given in Fig. 5 which, however, can only be interpreted on the basis of data of other systems which define less-disturbed reference distribution patterns. The Pilok, Thailand, and Hermyingyi, Burma, apogranites show a deficiency in tin and a scatter distribution when compared with the systematic tin enrichment trend in the Erzgebirge granite suite (Fig. 5b). The Erzgebirge reference suite is defined by a large sample population of regional distribution, whereas the Pilok and Hermyingyi sample populations are from apical portions of small granite stocks with pervasive alteration. The variation plot of Fig. 5a shows sample populations from the same systems for the Ta–Ti element pair. These two components are relatively immobile in hydrothermal systems and reflect the systematic magmatic enrichment of incompatible tantalum and systematic depletion in compatible titanium.

Large-scale scavenging of metals must of course not be limited to aqueous fluid phases. This can also be achieved by exsolution of hydro-carbo-thermal fluids in carbonatite systems which can transport large amounts of rare earth elements (Bühn and Rankin 1999). Another mechanism is exsolution of an immiscible sulphide melt which in mafic/ultramafic systems leads to large-scale depletion in chalcophile elements, such as nickel and platinum group elements, and complementary enrichment in the sulphide fraction of the system (Naldrett 1999). The density contrast to the silicate host system leads to upward movement of
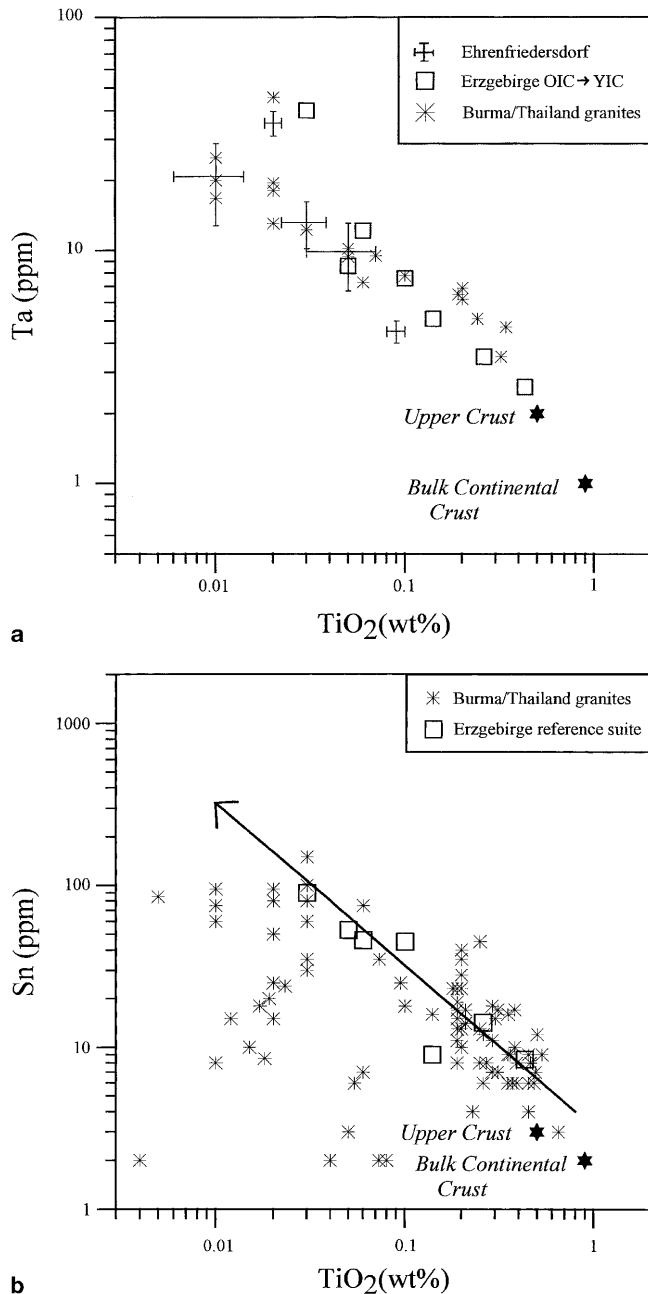
Fig. 5 TiO$_2$ vs **a** Ta (above) and **b** Sn (below) for bulk-rock samples from tin granites of the Pilok and Hermyingyi areas, Thailand–Burma border ranges, and from the Ehrenfriedersdorf tin granite, and the Erzgebirge granite reference suite (arithmetic means of a large sample number from Older granites 1–3, Younger granites 1–3, and Zinnwald. Data from Tischendorf (1989), Lehmann et al. (1994) and Schneider (1995)

aqueous metal-rich fluids, and to downward movement of sulphidic segregations, which is the reason for the apical position of hydrothermal ore deposits related to felsic magmatism, and the location of magmatic sulphide deposits near the base of igneous systems.

Ore environments

Silicic magmatism is the most important crust formation and intracrustal fractionation process. Several weight percent water are required for the formation of silicic melts under crustal conditions. Water is derived from dehydration of the lower crust and, more importantly, from subduction of hydrated oceanic crust. Melt emplacement in the upper crust leads to separation of volatile phases (first and second boiling, i.e. spontaneous vesiculation due to declining confining pressure, and increasing water content due to crystallization of anhydrous mineral phases, respectively) which interact with other waters forming a hydrothermal plume (Whitney 1975). Major types of ore deposits of Cu, Mo, Au, Ag, base and rare metals are related to this environment. In terms of decreasing magmatic input, these include pegmatite, porphyry/greisen, skarn, mesothermal, epithermal and exhalative massive sulphide systems. In the latter case, nearly all of the fluids involved are recycled seawater and the metals derive from high- and low-temperature water–rock interaction with little or no magmatic chemical input. On the contrary, the metal budget of porphyry systems is dominated by the associated magmatic systems, and controlled by the magmatic and magmatic–hydrothermal evolution of these systems.

Subduction and associated orogenic processes along growing continental margins produce extensive mid-crustal fluid flow (Goldfarb et al. 1991). Metamorphic devolatilization leads to low salinity H$_2$O–CO$_2$ fluids which become focussed in large-scale shear zones. Orogenic lode gold mineralization forms from such fluids mainly within a narrow temperature window of 400 to 300 °C (Loucks and Mavrogenes 1999).

Sedimentary basins host the major oil, gas, coal and evaporite deposits of the Earth, as well as important synsedimentary (banded and minette-type iron and manganese deposits, heavy-mineral placers, shale-hosted massive sulphide deposits) and diagenetic ore deposits (copper sandstone/shale, Mississippi Valley-type lead–zinc–fluorite–barite deposits, uranium roll-front and unconformity-type deposits; Eidel 1991). Mineral precipitation occurs along physicochemical interfaces, such as at the sea floor or in stratified water columns (synsedimentary ore formation), or in aquifers within basin fill (diagenetic ore formation from high-salinity basinal brines). Paleo-hydrology and basin stratigraphy control the lifetime of steady-state fluid flow and of the stationary solution interface (Klein 1991).

The existence of metallogenic provinces is evidence for the large-scale control of ore formation and the interplay between global tectonics, erosional history and palaeo-climate in any given region. The preservation probability of ore deposits, i.e. their age distribution, is again a function of their geodynamic setting (Veizer and Jansen 1979).

## Case study on porphyry systems: the Andean convergent margin

The Central Andes provide a textbook example of ore formation at convergent plate margins (Sillitoe 1976; Petersen 1999). The volcano-plutonic orogen of the Central Andes is constructed along an active plate margin between the overriding continental edge of South America and the subducting Pacific lithosphere. This general configuration appears to have been active since at least Permo-Triassic times. Ore formation in the Central Andes during the past 200–250 Ma is characterized by punctuated regional episodes on a general geotectonic background of quasi-continuous subduction along the South American convergent plate margin. Some of the most spectacular ore systems in this framework are the copper porphyry deposits of northern and central Chile, and the vein and porphyry deposits of the Andean tin belt of Bolivia and southernmost Peru. Both metal provinces represent short episodes of ore formation in narrow belts of more than 1000 km strike length, and approximately 300 km apart (Fig. 6). The most important Chilean copper porphyry systems developed in the time interval of 43 to 31 Ma (Collahuasi/Quebrada Blanca, Chuquicamata, La Escondida, El Salvador) and 10 to 4 Ma (Los Pelambres, Rio Blanco/Los Bronces, El Teniente; Sillitoe 1988; Clark et al. 1998). The Andean tin belt hosts minor ~ 220-Ma-old tin granite systems (Chacaltaya, Chojlla) and major world-class 25- to 12-Ma-old tin granite/porphyry systems (San Rafael, San José/Oruro, Llallagua, Cerro Rico de Potosi, Chorolque; Fig. 6; Grant et al. 1979; McBride et al. 1983; Sillitoe et al. 1975). The principal current tin producer of the region, also the world's single largest active tin mine, is the San Rafael Cu–Sn mine in SE Peru.

The two metal belts host both the largest individual copper and the largest individual tin resource in the world. The copper mineralized complex at Chuquicamata is approximately 14 km long, straddling the Domeyko or West Fissure fault, and includes the south-to-north mineralized zones at MM, Mina Sur (formerly Exotica), Chuquicamata, Chuqui Norte, and Radomiro Tomic. The total copper resource is > 11 billion tonnes of ore at 0.2 wt.% Cu cutoff grade, with an average grade of 0.76 wt.% Cu (Chávez 1999). This yields a total of > 84 million metric tonnes of contained Cu, of which production to date totals nearly 33 million metric tonnes Cu. The magnitude of the copper tonnage of the Chuquicamata complex of around 10^8 tonnes Cu requires leaching of a minimum rock mass of approximately 2.5×10^9 tonnes assuming an average copper content of 80 ppm Cu for volcanic-arc material (Stanton 1994) which equates to a cube of $50 \times 10 \times 10$ km. Given an efficiency of metal leaching of probably < 30%, this volume figure increases to more than $50 \times 10 \times 30$ km, i.e. large-scale copper redistribution on a 10-km scale must be involved in the formation of large copper porphyry systems.

The Llallagua tin porphyry system in Bolivia represents the largest individual tin ore system in the

Fig. 6 Major porphyry ore deposits in the Central Andes
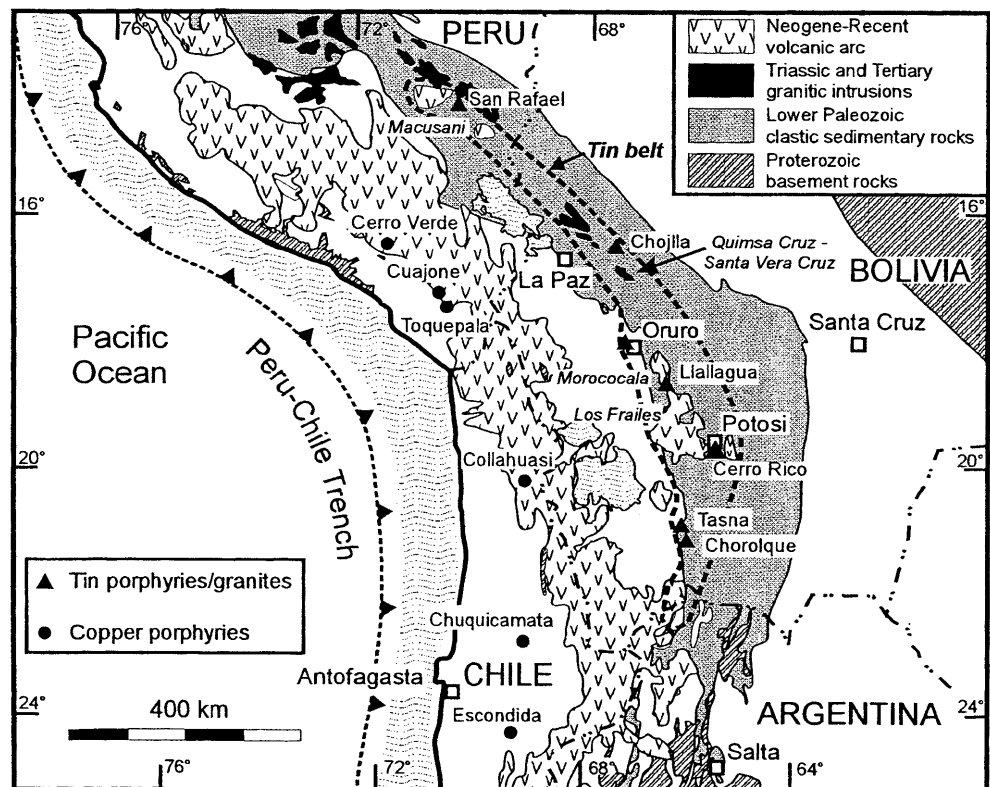
world. Its historic production is approximately 500,000 tonnes Sn, and the geochemical halo plus ore is estimated to include approximately 2 million metric tonnes Sn in a pipe-like stock with approximately 1 km² exposed surface (Dietrich et al. 1997). This metal content translates into a leached minimum rock volume of average continental crust of approximately 400 km³ with 2.5 ppm Sn (probably in a two-step process of magmatic tin enrichment and hydrothermal redistribution; see below). Therefore, ore formation under conditions of efficiency of metal leaching of probably < 30 % requires again a large-scale process with a rock volume involved of at least $4 \times 10 \times 30$ km.

Whereas the metallogeny of copper–porphyry belts is generally understood as a result of their convergent margin setting with subduction of oceanic lithosphere and partial melting of hydrated mantle-wedge material, the conceptual model for the metallogeny of tin is usually based on intracrustal melting and advanced degree of magmatic fractionation in high-silica systems (Lehmann 1990). An apparent exception are the Bolivian tin–porphyry systems which are associated with only moderately fractionated subvolcanic rocks of rhyodacitic composition.

We studied the geochemistry of the tin–porphyry systems of Llallagua, Cerro Rico de Potosi, and Chorolque in central and southern Bolivia. These systems range in age from 21 to 14 Ma and consist of rhyodacitic stocks and breccias with pervasive hydrothermal overprint (mainly sericitization, silicification, and tourmalinization; Grant et al. 1980; Sillitoe et al. 1975). The igneous rocks are composed of fine- to coarsegrained phenocrysts of feldspars, biotite, and strongly corroded quartz, set in a fine-grained matrix. Phenocrysts share approximately 40–50 % of the rock and are often broken to fine-grained fragments. The approximate primary phenocryst proportion is 35 % quartz, 50 % feldspars and 15 % biotite. Tin mineralization occurs as disseminated hydrothermal cassiterite and in quartz–tourmaline–cassiterite-sulphide veins.

The bulk-rock geochemistry of the porphyry systems defines a rhyodacitic to dacitic composition with moderate degree of fractionation (TiO_2 0.5–0.9 wt. %, Zr 100–300 ppm, Ta 1–4 ppm). Hydrothermal overprint has resulted in strong enrichment of B, Bi and Sn (> 100 times the upper continental crust), and in moderate enrichment of Sb, Pb, Ag, As, Au and W (10–100 times the upper continental crust).

Silicate melt inclusions in quartz phenocrysts were studied by electron and proton microprobe analysis (Dietrich 1999; Wallianos 1998). The melt inclusions have peraluminous composition; alkali and silica contents define a rhyolitic melt phase of high-K affinity. Major element composition reflects that crystallization occurred after fractionation of plagioclase and mafic phases, and prior to or concurrent with formation of alkali feldspar. The trace-element composition of the melt inclusions is distinctly different from the bulkrock geochemistry. Electron microprobe and PIXE data indicate a highly evolved melt with 0.03–0.12 wt. % TiO_2, 15–85 ppm Zr, 5–17 ppm Ta, 5–43 ppm Sn and Rb/Sr up to 60. Low Nb/Ta and Zr/Hf ratios of 2–6 and 3–11, respectively, are typical of highly fractionated tin granites and rare-element enriched pegmatites. The melt-inclusion data align with the general fractionation trend of Tertiary felsic rocks of the Andean tin belt, and are similar to the Macusani lithophile-element-enriched rhyolites, SE Peru, and to the most fractionated rocks in the Cordillera Quimsa Cruz tin granites of northern Bolivia (Fig. 7). The immobile-element bulk-rock data of the tin porphyries plot in between the upper-crust and bulk-crust reference points. The scatter distribution of the bulk-rock tin data reflects pervasive hydrothermal overprint.

Magmatic mixing

The compositional gap between the highly evolved nature of the melt inclusions and the intermediate bulk-rock geochemistry cannot be explained by crystal–liquid fractionation in a closed system. The amount of phenocrysts in the tin porphyries ranges between 40 and 50 %, which allows only an up to twofold enrichment of perfectly incompatible elements in a late-stage cogenetic melt phase. The correlation trends of Fig. 7 preclude any important influence of boundary-layer effects. The highly fractionated nature of the melt inclusions would require a phenocryst/melt ratio of > 4 which appears unrealistically high (Dietrich et al. 1999). In addition, the melt inclusions occur in quartz phenocrysts with strong magmatic corrosion features arguing against late quartz crystallization. We therefore propose an explanation by mixing of a highly evolved silicic melt, containing quartz phenocrysts, with andesitic to basaltic melt fractions in an upper crustal reservoir. Tin mineralization and boron metasomatism appear to be related to fluid exsolution from this inferred highly fractionated melt reservoir which could explain the exceptional association of tin mineralization with an only moderately fractionated bulk-rock system.

Mixing is also indicated by new neodymium isotope data from the Bolivian tin porphyries which range in ε_{Nd} from −5 to −10. The Lower Paleozoic country rocks and the Proterozoic basement have ε_{Nd} ranges of −8 to −12, and −11 to −14, respectively. These data suggest a largely intracrustal source but require some mantle input for the Bolivian tin porphyries (Lehmann et al. 2000).

The mixing process between mafic or andesitic melt and a high-silica melt may trigger a runaway mechanism of catastrophic volatile release and explosive venting in subvolcanic plutons (Anderson 1976). Large-scale vapour percolation can effectively sequester ore metals, given the favourable confluence of a number of critical chemical parameters such as
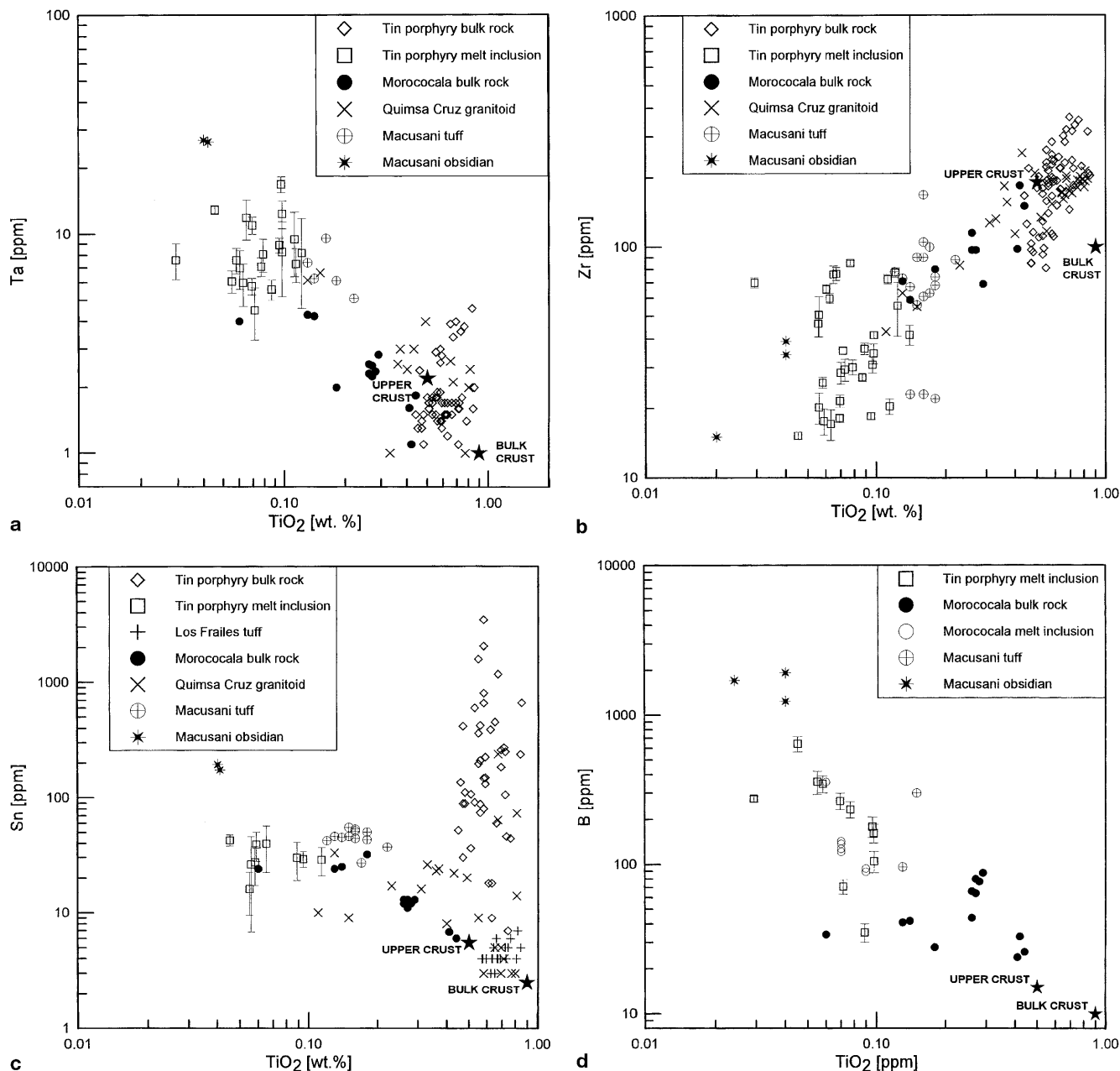
Fig. 7a–d TiO$_2$ vs Ta, Zr, Sn and B for bulk-rock samples and melt inclusions from tin porphyries of the Bolivian tin belt. Data from Dietrich (1999), Morgan et al. (1998) and Pichavant et al. (1987, 1988)

magma composition and oxidation state (Candela 1989). The punctuated evolution of devolatilizing composite magmatic systems may also be important in the evolution of the Chilean copper–molybdenum–gold porphyries for which Sr–Nd isotope data suggest magma mixing concomitant with hydrothermal breccia and ore formation (Skewes and Stern 1996).

Fractional crystallization and early exsolution of a magmatic vapour phase

The melt inclusions are enriched in incompatible elements such as boron, arsenic, cesium, tantalum, and are depleted in compatible components such as titanium and zirconium (Fig. 7). These trends apply both to volatile and non-volatile components and are therefore attributed to magmatic processes. The relatively high abundances of boron suggest input to the magmatic system by partial melting of boron-rich material, i.e. pelitic rocks. The linear correlation trends in log–log plots suggest fractional crystallization as the dominant petrogenetic process (Fig. 7). However, there are

two elements which deviate from systematic trends and which show random distributions. These elements are copper and silver (Fig. 8) which both have a bimodal frequency distribution. The copper data separate into a low-Cu population with a geometric mean of 2 ppm Cu (1–10 ppm Cu), and a high-Cu population with a geometric mean of 2000 ppm Cu (100–7000 ppm Cu). The former population consists of natural glassy melt inclusions, the latter one of remelted/rehomogenized melt inclusions. We infer that the

original copper content from the melt phase was lost to the vapour bubble during cooling. Rehomogenization redistributed the copper content from the vapour bubble into the glass phase, and quenching led to fixation of the copper in the melt phase. The original copper content of the melt system must, therefore, have been of the order of 2000 ppm Cu.

A similar pattern is seen for silver which has high abundances of 20–300 ppm Ag (geometric mean: 60 ppm Ag) in rehomogenized/remelted melt inclusions. Silver in natural glassy melt inclusions is below the analytical PIXE detection limit of around 10 ppm Ag. Following the foregoing reasoning for copper, the melt system must also have had silver contents of the order of 60 ppm Ag. This is an enrichment factor for both copper and silver of around 100 when compared with average upper crust.

The scatter distribution for both Cu and Ag must be attributed to a volatile phase which is thought to have transported these two elements into the melt system. We conclude that the melt inclusions both record a closed-system intramagmatic fractionation trend (most elements) and ingress of volatiles in an open system (copper and silver). A strong preference of copper for magmatic volatile phases is known from other silicic systems (Lowenstern et al. 1991), with copper partitioning preferentially into the vapour relative to the brine in sub-solidus vapour-brine systems (Ulrich et al. 1999). The exceptionally high copper and silver abundances require an efficient concentration mechanism likely to be volatile stripping by a vapour phase from a large volume of mantle-derived melt underlying the rhyolitic melt portions recorded in the melt inclusions. Magmatic mixing is known to easily trigger volatile exsolution (Sparks et al. 1977; Huppert et al. 1982).

Mafic-to-silicic volatile transfer processes have also been suggested for the formation of molybdenum porphyries which in apical portions have very high magmatic Mo abundances (Keith and Shanks 1988; Carten et al. 1988). Volatile stripping may have helped transform Mo-poor magma (3 ppm) into Mo-rich magma (>1000 ppm) which on subsequent crystallization yielded a concentrated ore fluid (Keith et al. 1998).

It is interesting to note that the high-Ag signature is not only seen in the well-known silver deposit of Cerro Rico de Potosi, but is just as well developed in the Llallagua tin porphyry. Llallagua has a deeper erosion level than Cerro Rico, and has no silver mineralization. It appears that the potential for Ag mineralization was developed in Llallagua, with the epithermal and possibly Ag-rich cap eroded.

The high-Cu signature in the melt inclusions studied is not related to any known important copper mineralization, although copper is enriched in some Bolivian vein systems. However, the association of copper and tin is typical of the Cornwall province (Halls 1994) and the W–Sn–Cu Sanyo belt in Japan (Ishihara 1981). The principal current tin producer in the
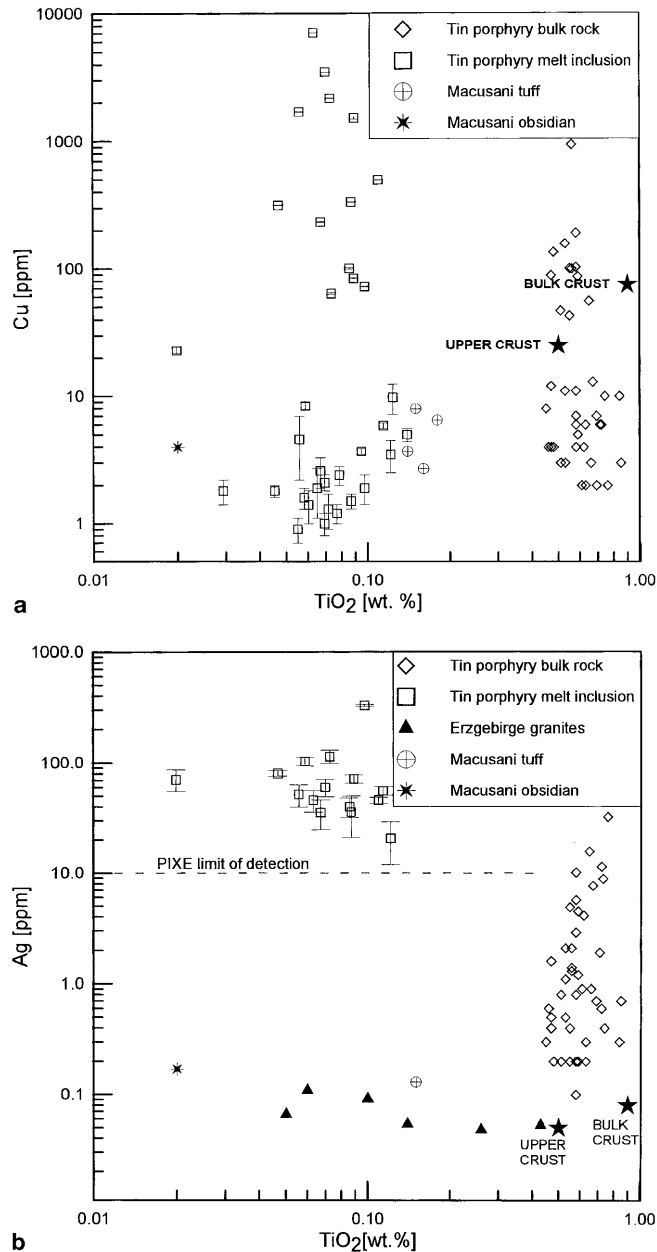

Fig. 8a,b TiO_2 vs Cu (above) and Ag (below) in bulk-rock samples and melt inclusions from Bolivian tin porphyry systems. High-Cu and high-Ag populations are from remelted/rehomogenized melt inclusions in which vapour-phase components are quenched into glass fraction. Data from Dietrich (1999), Morgan et al. (1998) and Pichavant et al. (1987, 1988)

Andean tin belt, the San Rafael mine in SE Peru, was initially a copper mine and displays a large-scale hydrothermal zonation with copper enrichment on top of the system, and with tin enrichment in deeper parts. It appears that the copper potential seen in the Bolivian melt inclusions could not develop into large-scale copper mineralization, whereas the Chilean systems provided better conditions of postmagmatic copper focussing and fixation. Hydrothermal copper mobility is largely controlled by oxidation state (fH_2S/fSO_2), with much higher Cu solubility (chloride complexed) in oxidized fluid systems buffered by magnetite-series copper porphyry systems than by reduced ilmenite-series tin porphyry systems, whereas bisulphide-complexed copper has the opposite behaviour (Crerar and Barnes 1976). Hydrothermal copper in the Bolivian tin porphyry systems was apparently more mobile than in copper porphyry systems and became fixed at lower temperature and spatially separated from tin mineralization.

General model for porphyry ore systems

The metallogenic evolution of porphyry systems can be summarized in the following scheme:

1. Melt generation as a result of partial melting of hydrated mantle-wedge material, long-lived diffuse injection of basaltic melt into continental crust with hybridization and crustal mobilization (sensu Hildreth 1981) leads to a general andesitic–dacitic melt composition.
2. Emplacement into the upper crust and fractional crystallization with development of zoned magma chambers. Reaction progress is a function of crustal thickness. Long-term thermal preparation may allow partial melting of upper crustal material. Shale source material imprints high boron signature and eventually reducing melt character (ilmenite series).
3. Early exsolution of magmatic vapour phases (first boiling) from deeper and more mafic parts of the system with large-scale volatile stripping of copper and silver (probably also gold, not detectable by current microanalytical techniques).
4. Extended fractional crystallization in apical rhyolitic portions of magma system with systematic magmatic enrichment of tin and other incompatible components such as arsenic, boron, cesium, tantalum and tungsten with concomitant depletion in compatible components such as zirconium and titanium. Water saturation is depressed by high boron levels, and closed-system fractional crystallization is overlapped by ingress and redissolution of Cu- and Ag-rich volatile phases from lower parts of the system which leads to imprint of scatter distribution for the early vapour-phase-transported elements on highly fractionated melt portions.

5. Decompression during volcanic venting with catastrophic volatile release from large parts of the magma chamber. Volatile fluids are channeled and focussed by volcanic vent structure and imprint hydrothermal alteration/mineralization on subvolcanic host rocks. Tin-boron component is fixed in the central parts of the hydrothermal system, copper and silver/gold are more mobile and form an outer halo in tin porphyry systems (see also Cornwall).

Major ingredients of this model are the degree of fractional crystallization, the oxidation state and the volatile budget. Incorporation of boron in the granitic melts allows enhanced water contents in the magma and a proportional increase in mechanical energy available from expansion at the transitional magmatic–hydrothermal stage (Halls 1994).

A conceptual model is shown in Fig. 9 which combines experimental element distribution data on melt–crystal–fluid phase systems (Sn-W, Mo, Cu, Au-Ag) with our melt-inclusion data. The metallogeny of copper in porphyry systems is defined by mantle-induced partial melting and hybridization, and the early
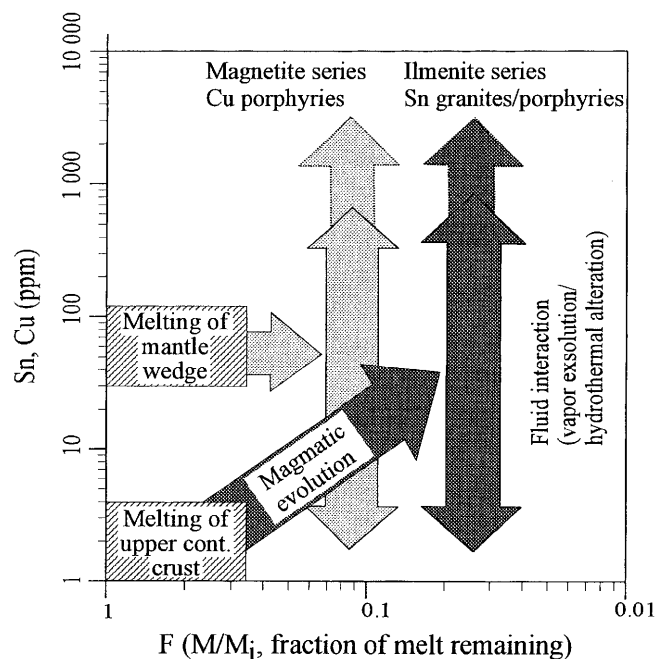

Fig. 9 Metallogenic model of tin and copper porphyry ore formation. Tin-bearing systems (dark shaded) are characterized by extended fractional crystallization and subsequent hydrothermal redistribution under low fO_2 conditions in order to allow Sn^{2+} as dominant tin species. Copper is scavenged in magnetite and biotite during fractional crystallization, which is why early vapour-phase exsolution will favour copper enrichment in the vapour phase. Silver and (by inference) gold follow the same vapour-controlled mobilization pattern. Tin and boron are enriched in late magmatic phases and are mobilized through magmatic brines. Note that tin and copper porphyry systems are part of the same continuum of lithospheric magmatism with variable degrees of interaction of mantle-derived magmas with continental crust

evolution of a magmatic vapour phase under high fO_2 conditions (magnetite series). The high fO_2 (and correspondingly high fSO_2) signature leads to sub-solidus iron oxidation with magnetite formation from iron-bearing silicates, and production of abundant H_2S which becomes fixed in pyrite so typical of copper porphyries (Takagi and Tsukumura 1997). Crystal fractionation processes and concomitant sulphide immiscibility tend to decrease copper and gold/silver content in the silicate melt system which is why exsolution of an early magmatic vapour phase is probably instrumental for effective volatile enrichment of copper and gold–silver. Advanced degree of fractionation in hybrid upper crustal magma chambers can lead to enrichment of molybdenum within the same magnetite-series high fO_2 system. Magmatic enrichment of tin requires reducing conditions in a low fO_2 system (ilmenite series) which can be produced by partial melting of upper crustal shale material. The opposite redox sensitivity in the crystal–melt and solid–fluid partitioning behaviour of molybdenum and tin leads to two mainly mutually exclusive ore environments (Lehmann 1990). Tungsten can be enriched in both oxidizing and reducing environments (Candela and Bouton 1992).

The Bolivian porphyries have both features of copper porphyry systems and of tin granites. Their geotectonic setting in thick back-arc continental crust has diluted the initially mantle-dominated magmatic situation which is still largely preserved in the Chilean copper porphyry systems. Instead, large-scale upper crustal melting has strongly modified the melt systems and allowed advanced degree of fractionation under low fO_2 conditions. The roots of the Bolivian porphyry systems are supposed to be magnetite-series gabbroic–dacitic melts similar to copper porphyry systems, whereas the upper parts of the melt systems are controlled by upper crustal partial melts of ilmenite-series affinity. This hybrid character is typical of the Bolivian tin province but may also apply to other ore provinces which have both tin and copper enrichment, such as Cornwall. The porphyry ore spectrum reflects the general petrological spectrum of lithospheric magmatism in which mantle-derived magmas supply heat and mass to crustal systems that evolve a variety of compositional ranges through fractionation and assimilation.

Attainment of ore grade in shallow parts of porphyry systems reflects repetitive fluid focussing and extreme degree of fluid–rock metasomatism. The interplay between explosive venting, decompression and catastrophic volatile release may establish a runaway mechanism able to efficiently extract volatile phases from deep portions of stratified magmatic systems. Volatile stripping of copper and silver (and gold, by inference) by early magmatic vapour phases from less evolved melt portions, and extraction of chloride-complexed metals, such as tin by brine exsolution from highly evolved melt fractions, are superimposed and reflect the hybrid character of the underlying melt systems.

References

Allègre CJ, Manhès G, Göpel C (1995) The age of the Earth. Geochim Cosmochim Acta 59:1445–1456

Anders E, Grevesse N (1989) Abundances of the elements: meteoritic and solar. Gochim Cosmochim Acta 53:197–214

Anderson AT (1976) Magma mixing: petrological process and volcanological tool. J Volcanol Geotherm Res 1:3–33

Brimhall GH Jr (1987) Preliminary fractionation patterns of ore metals through Earth history. Chem Geol 64:1–16

Bühn B, Rankin AH (1999) Composition of natural, volatile-rich Na–Ca–REE–Sr carbonatitic fluids trapped in fluid inclusions. Geochim Cosmochim Acta 63:3781–3797

Campbell IR, Taylor SR (1983) No water, no granites – no oceans, no continents. Geophys Res Lett 10:1061–1064

Candela PA (1989) Felsic magmas, volatiles, and metallogenesis. Rev Econ Geol 4:223–233

Candela PA, Bouton SL (1992) The influence of oxygen fugacity on tungsten and molybdenum partitioning between silicate melts and ilmenite. Econ Geol 633–640

Carten RB, Geraghty EP, Walker BM, Shannon JR (1988) Cyclic development of igneous features and their relationship to high-temperature hydrothermal features in the Henderson porphyry molybdenum deposit, Colorado. Econ Geol 83:266–296

Chávez WX (1999) Exploration review: Chile. Soc Econ Geol Newslett 35:24–26

Clark AH, Archibald DA, Lee AW, Farrar E, Hodgson CJ (1998) Laser probe 40Ar/39Ar ages of early and late-stage alteration assemblages, Rosario porphyry copper–molybdenum deposit, Collahuasi district, I Region, Chile. Econ Geol 93:326–337

Cox A, Hart RB (1986) Plate tectonics: how it works. Blackwell, Oxford, pp 1–392

Crerar DA, Barnes HL (1976) Ore solution chemistry. V. Solubilities of chalcopyrite and chalcocite assemblages in hydrothermal solution at 200° to 350 °C. Econ Geol 71:772–794

Dietrich A (1999) Metallogenie, Geochemie und Schmelzeinschluss-Untersuchungen von tin porphyry und copper porphyry Lagerstätten der zentralen Anden (Bolivien, Chile). Clausthaler Geowiss Diss 57:1–198

Dietrich A, Lehmann B, Wallianos A, Traxel K (1997) The Lower Miocene tin porphyry system of Llallagua, Bolivia: bulk rock and melt inclusion geochemistry. In: Papunen H (ed) Mineral deposits. Balkema, Rotterdam, pp 625–628

Dietrich A, Lehmann B, Wallianos A, Traxel K, Palacios C (1999) Magma mixing in Bolivian tin porphyries. Naturwissenschaften 86:40–43

Dietrich A, Lehmann B, Wallianos A (in press) Bulk rock and melt inclusion geochemistry of Bolivian tin porphyry systems. Econ Geol

Eidel JJ (1991) Basin analysis for the mineral industry. Rev Econ Geol 5:1–15

Geochemical Earth Reference Model (1998) http://www-ep.es.llnl.gov/germ

Goldfarb RJ, Snee LW, Miller LD, Newberry RJ (1991) Rapid dewatering of the crust deduced from ages of mesothermal gold deposits. Nature 354:296–298

Grant JN, Halls C, Avila W, Snelling NJ (1979) K–Ar ages of igneous rocks and mineralization in part of the Bolivian tin belt. Econ Geol 74:838–851

Grant JN, Halls C, Sheppard SMF, Avila W (1980) Evolution of the porphyry tin deposits of Bolivia. Mining Geol Spec Issue 8:151–173

Groves DI (1993) The crustal continuum model for late-Archean lode-gold deposits of the Yilgarn Block, Western Australia. Mineral Deposit 28:366–374

Halls C (1994) Energy and mechanism in the magmatic-hydrothermal evolution of the Cornubian batholith: a review. In: Seltmann R, Kämpf H, Möller P (eds) Metallogeny of collisional orogens. Czech Geol Surv, Prague, pp 274–294

Helgeson HC (1964) Complexing and hydrothermal ore deposition. Pergamon, Oxford, pp 1–128

Hildreth W (1981) Gradients in silicic magma chambers: implications for lithospheric magmatism. J Geophys Res 86:10153–10192

Holland HD (1967) Gangue minerals in hydrothermal deposits. In: Barnes HL (ed) Geochemistry of hydrothermal ore deposits. Holt Rinehart Winston, New York, pp 382–436

Huppert HE, Sparks RSJ, Turner JS (1982) Effects of volatiles on mixing in calc-alkaline magma systems. Nature 297:554–557

Ishihara S (1981) The granitoid series and mineralization. Econ Geol 75th Anniv Vol: 458–484

Keith JD, Shanks WC (1988) Chemical evolution and volatile fugacities of the Pine Grove porphyry molybdenum and ash-flow tuff system, southwestern Utah. CIM Spec Vol 39:402–423

Keith JD, Christiansen EH, Maughan DT, Waite KA (1998) The role of mafic alkaline magmas in felsic porphyry-Cu and Mo systems. Mineral Assoc Can Short Course Series 26:211–243

Klein G deV (1991) Rationale for modern basin analysis applied to ore deposits. Rev Econ Geol 5:21–23

Lehmann B (1990) Metallogeny of tin. Springer, Berlin Heidelberg New York, pp 1–211

Lehmann B (1994) Globale chemische Fraktionierungstrends und Lagerstättenbildung. Naturwissenschaften 81:108–114

Lehmann B, Yungyusuk N, Khositanont S, Höhndorf A, Kuroda Y (1994) The tin-tungsten ore system of Pilok, Thailand. J Southeast Asian Earth Sci 10:51–63

Lehmann B, Dietrich A, Heinhorst J, Métrich N, Mosbah M, Palacios C, Schneider H-J, Wallianos A, Webster J, Winkelmann L (2000) Boron in the Bolivian tin belt. Mineral Deposit 35:223–232

Loucks RR, Mavrogenes JA (1999) Gold solubility in supercritical hydrothermal brines measured in synthetic fluid inclusions. Science 284:2159–2163

Lowenstern JB, Mahood GA, Rivers ML, Sutton SR (1991) Evidence for extreme partitioning of copper into a magmatic vapor phase. Nature 252:1405–1409

McBride SL, Robertson RCR, Clark AH, Farrar E (1983) Magmatic and metallogenetic episodes in the northern tin belt, Cordillera Real, Bolivia. Geol Rundsch 72:685–713

McDonough WF, Sun SS (1995) The composition of the Earth. Chem Geol 120:223–253

Mitchell AHG, Garson MS (1981) Mineral deposits and global tectonic settings. Academic Press, London, pp 1–405

Morgan JW, Anders E (1980) Chemical composition of Earth, Venus, and Mercury. Proc Natl Acad Sci USA 77:6973–6977

Morgan GB, London D, Luedke RG (1998) Petrochemistry of Late Miocene peraluminous silicic volcanic rocks from the Morococala field, Bolivia. J Petrol 39:601–632

Naldrett AJ (1999) World-class Ni–Cu–PGE deposits: key factors in their genesis. Mineral Deposit 34:227–240

Nozaki Y (1997) A fresh look at element distribution in the North Pacific. http://earth.agu.org/eos-elec/

Palme H, O'Neill SC (1996) Formation of the Earth's core. Geochim Cosmochim Acta 60:1106–1108

Petersen U (1999) Magmatic and metallogenic evolution of the Central Andes. Soc Econ Geol Spec Publ 7:109–153

Pichavant M, Herrera JV, Boulmier S, Brique L, Joron JL, Juteau M, Marin L, Michard A, Sheppard SMF, Treuil M, Vernet M (1987) The Macusani glasses, SE Peru: evidence of chemical fractionation in peraluminous magmas. In: Mysen BO (ed) Magmatic processes: physicochemical principles. Geochem Soc Spec Publ 1:359–373

Pichavant M, Kontak DJ, Brique L, Herrera JV, Clark AH (1988) The Miocene–Pliocene Macusani volcanics, SE Peru. Contrib Mineral Petrol 100:300–338

Schneider T (1995) Petrographie und Geochemie des Granit-Pegmatit-Aplitsystems von Ehrenfriedersdorf im Erzgebirge. MSc thesis, TU Clausthal, pp 1–114

Sillitoe RH (1976) Andean mineralization: a model for the metallogeny of convergent plate margins. Geol Assoc Can Spec Pap 14:59–100

Sillitoe RH (1988) Epochs of intrusion-related copper mineralization in the Andes. J South Am Earth Sci 1:89–108

Sillitoe RH (1997) Characteristics and controls of the largest porphyry Cu–Au and epithermal gold deposits in the circum-Pacific region. Austral J Earth Sci 44:373–388

Sillitoe RH, Halls C, Grant JN (1975) Porphyry tin deposits in Bolivia. Econ Geol 70:913–927

Skewes MA, Stern CR (1996) Late Miocene mineralized breccias in the Andes of Central Chile: Sr- and Nd-isotopic evidence for multiple magmatic sources. In: Camus F, Sillitoe RH, Petersen R (eds) Andean copper deposits: new discoveries, mineralization, styles and metallogeny. Soc Econ Geol Spec Publ 5:33–42

Sparks SRJ, Sigurdsson H, Wilson L (1977) Magma mixing: a mechanism for triggering acid explosive eruptions. Nature 267:315–318

Stanton RL (1994) Ore elements in arc lavas. Clarendon Press, Oxford, pp 1–391

Takagi T, Tsukumura K (1997) Genesis of oxidized- and reduced-type granites. Econ Geol 92:81–86

Taylor SR (1992) Solar system evolution. A new perspective. Cambridge University Press, Cambridge, pp 1–307

Taylor SR, McLennan SM (1985) The continental crust: its composition and evolution. Blackwell, Oxford, pp 1–312

Tischendorf G (1989) Silicic magmatism and metallogenesis of the Erzgebirge (compiled by G. Tischendorf). Veröffentl Zentralinst Physik Erde (Potsdam)107:1–316

Ulrich T, Günther D, Heinrich CA (1999) Gold concentrations of magmatic brines and the metal budget of porphyry copper deposits. Nature 399:676–679

Veizer J, Jansen SL (1979) Basement and sedimentary recycling and continental evolution. J Geol 87:341–370

Wallianos A (1998) Mikroanalytik an magmatischen Schmelzeinschluessen und spezielle Probleme bei der Datenauswertung von PIXE-Spektren. PhD thesis, Univ Heidelberg, pp 1–125

Wedepohl KH (1995) The composition of the continental crust. Geochim Cosmochim Acta 59:1217–1232

Whitney JA (1975) Vapor generation in a quartz monzonite magma: a synthetic model with application to porphyry copper deposits. Econ Geol 70:346–358

Zhang Y (1998) The young age of Earth. Geochim Cosmochim Acta 62:3185–3189